

# Gold nanoparticle probe-based gene expression analysis with unamplified total human RNA

Martin Huber, Tai-Fen Wei, Uwe R. Müller, Phil A. Lefebvre, Sudhakar S. Marla and Y. Paul Bao\*

Nanosphere Inc., 4088 Commercial Ave., Northbrook, IL 60062, USA

Received July 6, 2004; Revised and Accepted September 13, 2004

## ABSTRACT

**Microarray-based gene expression analysis plays a pivotal role in modern biology and is poised to enter the field of molecular diagnostics. Current microarray-based gene expression systems typically require enzymatic conversion of mRNA into labeled cDNA or cRNA. Conversion to cRNA involves a target amplification step that overcomes the low sensitivity associated with commonly used fluorescent detection methods. Herein, we present a novel enzyme-free, microarray-based gene expression system that uses unamplified total human RNA sample as the target nucleic acid. The detection of microarray-bound RNA molecules is accomplished by targeting the poly-A tail with an oligo-dT<sub>20</sub> modified gold nanoparticle probe, signal amplification by autometallography, and subsequent measurement of nanoparticle-mediated light scattering. The high sensitivity afforded by the nanoparticle probes allows differential gene expression from as little as 0.5 µg unamplified total human RNA in a 2 h hybridization without the need for elaborate sample labeling steps.**

## INTRODUCTION

Monitoring gene expression levels by using microarrays has evolved into a widely accepted tool in the research community, and is about to enter the diagnostic market (1). Microarrays have tremendously improved our understanding of the complex network of gene expression and its regulation in different cells and tissues (2,3). Concomitantly, this knowledge has provided insight into the mechanism of complex diseases and may pave the way for novel therapeutic approaches (4–8). For instance, characterization of tumors based on their unique expression profile may help guide adjustments in treatment and improve the outcome of therapy (9). However, significant technical and cost issues with present microarray-based gene expression analysis hamper the widespread use of this technology, especially in the cost-conscious clinical setting. Expression analysis typically requires target labeling for which direct and indirect methods are available. Indirect labeling is achieved by reverse transcribing the RNA sample to

incorporate fluorescently labeled nucleotides into the growing cDNA strand. The labeled cDNA is used as target in a microarray hybridization assay. In cases of limiting starting material, labeling of cDNA may not produce enough target molecules, requiring an *in vitro* transcription (IVT) amplification step (10). These cost and labor-intensive target preparation steps may also account, in part, for the described variability in microarray gene expression data (11,12). In contrast, direct labeling of RNA does not include an amplification step but utilizes enzymatic or chemical labeling of the RNA target (13–15). In cases of internal labels, the hybridization efficiency may be impaired due to a lower binding affinity between the target and capture probes (16). Another drawback of the direct labeling approaches is the lower sensitivity (minimum RNA requirement is 10 µg) due to the lack of target amplification steps.

We present a novel approach (ClearRead™) that also utilizes total human RNA as target nucleic acid, but in contrast to the above-mentioned methods, it does not require labeling or amplification steps for target preparation. After hybridizing the RNA to an oligonucleotide microarray, bound molecules are detected in a second hybridization step using oligonucleotide (oligo-dT<sub>20</sub>)-modified gold nanoparticle probes. These probes hybridize via their oligo-dT<sub>20</sub> sequences to the poly-A tail of captured mRNA molecules. The poly-A tail is a unique feature of eukaryotic mRNA molecules (except the animal histone mRNAs), conferring an increased stability to the mRNA in the cytoplasm (17). Ribosomal transcripts, which comprise the most abundant source of RNA in the cell, also lack the poly-A tail. Consequently, the oligo-dT<sub>20</sub> nanoparticles specifically detect only expressed coding sequences. After sufficient washes to remove unbound material, the light scatter ability of the gold nanoparticles is improved by autometallography: a brief step whereby Ag<sup>+</sup> ions are reduced to elementary silver that deposit around the Au particles. The resulting silver-amplified gold particles have a significantly increased extinction coefficient, leading to an approximately 1000-fold increase of their scatter signal (18). The resulting scatter light is captured by the photosensor of an imaging system (Verigene ID) specifically designed for scatter analysis (Figure 1). Scatter analysis has been previously shown to be on the order of 1000 times more sensitive than fluorescent-based detection methodologies (18). By applying this sensitive tool to gene expression analysis, we were able to detect low-expressed genes in 0.5 µg of unamplified total human RNA in a 2 h hybridization assay.

\*To whom correspondence should be addressed. Tel: +1 847 400 9150; Fax: +1 847 400 9199; Email: pbao@nanosphere.us

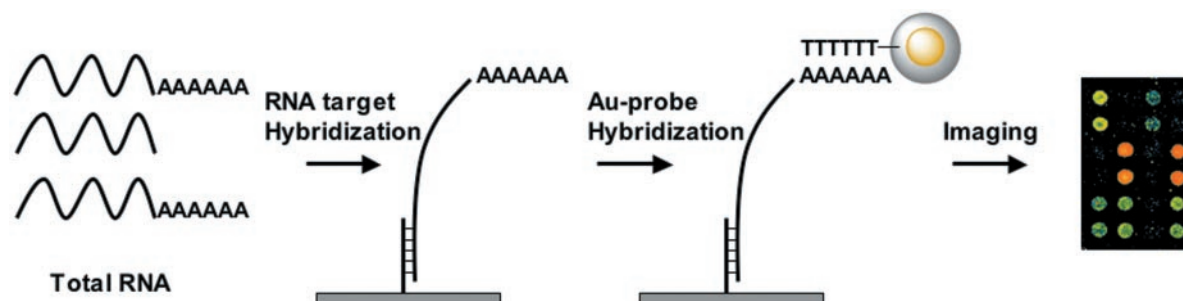


**Figure 1.** Schematic drawing of the ClearRead™ assay. Total human RNA is hybridized to complementary oligonucleotides attached to a microarray slide. In a second hybridization step, an oligo-dT<sub>20</sub>-modified gold nanoparticle probe is hybridized to the poly-A tail of the captured mRNA. Following silver enhancement, the slide is imaged using an in-house developed scanner (Verigene ID).

## MATERIALS AND METHODS

### Array preparation

All solutions were made in RNase-free plasticware (Nalge Nunc International, Rochester, NY; Brinkmann, Westbury, NY) using RNase-free water (Sigma, St Louis, MO). Capture probe oligos for human (The Midland Certified Reagent Company, Inc, Midland, TX) or bacterial (Ambion, Inc., Austin, TX) mRNA, designed to be complementary to the 3' end of the transcripts of interest, were diluted to 30  $\mu$ M in 150 mM sodium phosphate (Sigma) buffer containing 0.01% SDS (Fisher Scientific, Hampton, NH). Capture oligos were printed onto CodeLink slides (Amersham Bioscience, Piscataway, NJ) using an OmniGrid Accent arrayer (Genomic Solutions, Ann Arbor, MI), and the arrayed slides were stored at  $\geq 75\%$  humidity overnight to induce capture oligonucleotide attachment, then stored desiccated at RT until further use. Immediately prior to use, arrayed slides were soaked in 0.2% SDS for at least 10 minutes at 50°C then rinsed with water and dried. A plastic gasket (Grace Bio-Labs, Bend, OR) was applied to each sub-array to create a hybridization chamber.

### Nanoparticle preparation

Gold nanoparticles (~15 nm diameter) were prepared by the citrate reduction method (19). The approximate concentration of the gold nanoparticles was deduced from equating particle size measurements obtained by transmission electron microscopy (TEM) to the gold atom concentration, which was obtained by inductive coupled plasma-atomic emission spectroscopy (ICP-AES). Optical spectra ( $\lambda_{\text{max}} = 518$  nm) of the gold nanoparticles were recorded with an HP8453 UV-VIS spectrophotometer (Agilent Technologies, Palo Alto, CA). The oligonucleotide-modified gold nanoparticle probes were synthesized following protocols described previously (20). Briefly, 5' thiol-functionalized dT<sub>20</sub>-oligonucleotides (4  $\mu$ M final concentration) were initially incubated with gold nanoparticles for >16 h, followed by successive additions of phosphate buffered-NaCl (Sigma) to a final concentration of 0.8 M NaCl. After an overnight incubation, the probes were isolated by centrifugation, washed in an equivalent amount of water, then resuspended in a 0.1 M NaCl, 10 mM phosphate buffer pH 7, 0.01% sodium azide (Sigma) buffer at a particle concentration of 10 nM. Nanoparticle probes were stored at 4°C.

### RNA hybridization

Various concentrations of human total brain RNA (BD Biosciences, Palo Alto, CA) or synthetically 3' polyadenylated bacterial RNA (Ambion) were added to the hybridization buffer containing 4 $\times$  SSC (Invitrogen, Carlsbad, CA), 0.01% SDS, 0.04% sorbitan mono-9-octadecenoate poly(oxy-1,1-ethanediyl) (Tween-20™, Sigma) and 45% formamide (Sigma), and applied to the microarray. The arrays were incubated for 2 h at 40°C in a hybridization oven. After the indicated incubation period, the gasket was removed and the slide was soaked three times in wash buffer [0.5 N NaNO<sub>3</sub> (Sigma), 0.01% SDS and 0.02% Tween-20], rinsed in 4 $\times$  SSC and dried. The oligo-dT<sub>20</sub> nanoparticle probe (1 nM), in probe hybridization buffer (4 $\times$  SSC, 0.01% SDS, 0.04% Tween-20 and 25% formamide), was injected into new hybridization chambers and the slide incubated for 30 min at 40°C. Slides were soaked three times in wash buffer and once in 0.5 N NaNO<sub>3</sub>. Washed slides were stained with 2 ml of silver reagent, an admix of Silver Enhancer A and B solutions (Sigma) for 5.5 min, washed in ddH<sub>2</sub>O and dried. The slide was imaged with a Verigene ID™ imaging system (Nanosphere, Inc.). Red light-emitting diodes (LEDs) provide illumination of the slide creating an evanescent field in the glass slide. The resulting scatter signal of the silver-enhanced gold nanoparticles is captured on a photosensor and converted to a TIFF image. The dynamic range of the Verigene ID has been shown previously to be 2–3 logs, which is comparable to fluorescent scanners (18). The resulting images were further analyzed using the GenePix 5 software package (Axon Instruments, Union City, CA).

## RESULTS

### Sensitivity of ClearRead™

We have determined the minimum detectable RNA concentration by titrating four different *in vitro* transcribed bacterial RNAs that contained an artificially added poly-A tail. For this purpose, complementary 50mer capture oligonucleotides were printed at 30  $\mu$ M concentration onto CodeLink slides as described. RNA concentrations in the hybridization mixtures ranged from 0.1 pg to 1 ng, which is equivalent to an absolute number of  $2 \times 10^5$  to  $2 \times 10^9$  molecules in a total volume of 32  $\mu$ l. Hybridization conditions included a high-salt buffer

(4× SSC, 0.01% SDS, 0.04% Tween-20, 45% Formamide) and an incubation time of 2 h at 40°C. After removal of unbound nucleic acid, the oligo-dT<sub>20</sub> gold nanoparticle probe was applied to the microarray for hybridization under essentially the same conditions as used for the RNA hybridization, except that the Formamide concentration was lowered to 25%. Figure 2 shows that at 1 pg (2.9 amol) target concentration, all four RNA species exhibited signal intensities significantly higher than the control spots. Captures representing the human genes ubiquitin B and  $\beta$ -actin (UBB, ACTB) served as control spots in this experiment. Their net signals (mean signal corrected for the local background) were averaged, and after adding 1 SD, the resulting values were used as threshold for a positive signal call. In order to directly compare the data obtained at different scan times, net signals were normalized according to the different exposure times at which the images of different target concentrations were acquired. Normalization was accomplished by multiplying the net signal intensity by the ratio of the highest exposure time (800 ms) to the exposure time at which the image was captured. For example, the normalization factor for the 20 ms image is calculated as follows:  $800/20 = 40$ . The resulting relative signal values were plotted in a logarithmic scale (Figure 2B). At 0.1 pg target RNA concentration, signals dropped below the

threshold for a positive call. According to this data, we determined the minimum detectable target concentration to be 2.9 amol per hybridization. As a control we performed an assay without target RNA, which resulted in no detectable signal at any spot.

In other words, the gold nanoparticle probe-based expression system is capable of detecting  $\leq 55\,000$  RNA molecules/ $\mu$ l hybridization mix in a 2 h hybridization assay. This number is >10 times lower than a previously described detection limit of 60 amol for an overnight fluorescent-based hybridizations to a 60mer oligonucleotide array (21). Although each of the tested genes shows a linear dose response, the absolute signal intensities vary between different target spots (e.g. compare RNA#3 to RNA#2). This could be explained by differences in the secondary structures between target and/or capture molecules, resulting in different hybridization efficiencies. While this is of little consequence for the ratio determination of differential gene expression analysis, a careful design of the capture sequence could further improve the detection limit for individual genes. The fact that only a >10-fold increase in detection limit was found while the relative scatter signal from an amplified nanoparticle is  $\sim 1000$  times stronger than the relative fluorescence signal from a single fluorophore has an additional explanation: Typical 500 nt long cDNAs may

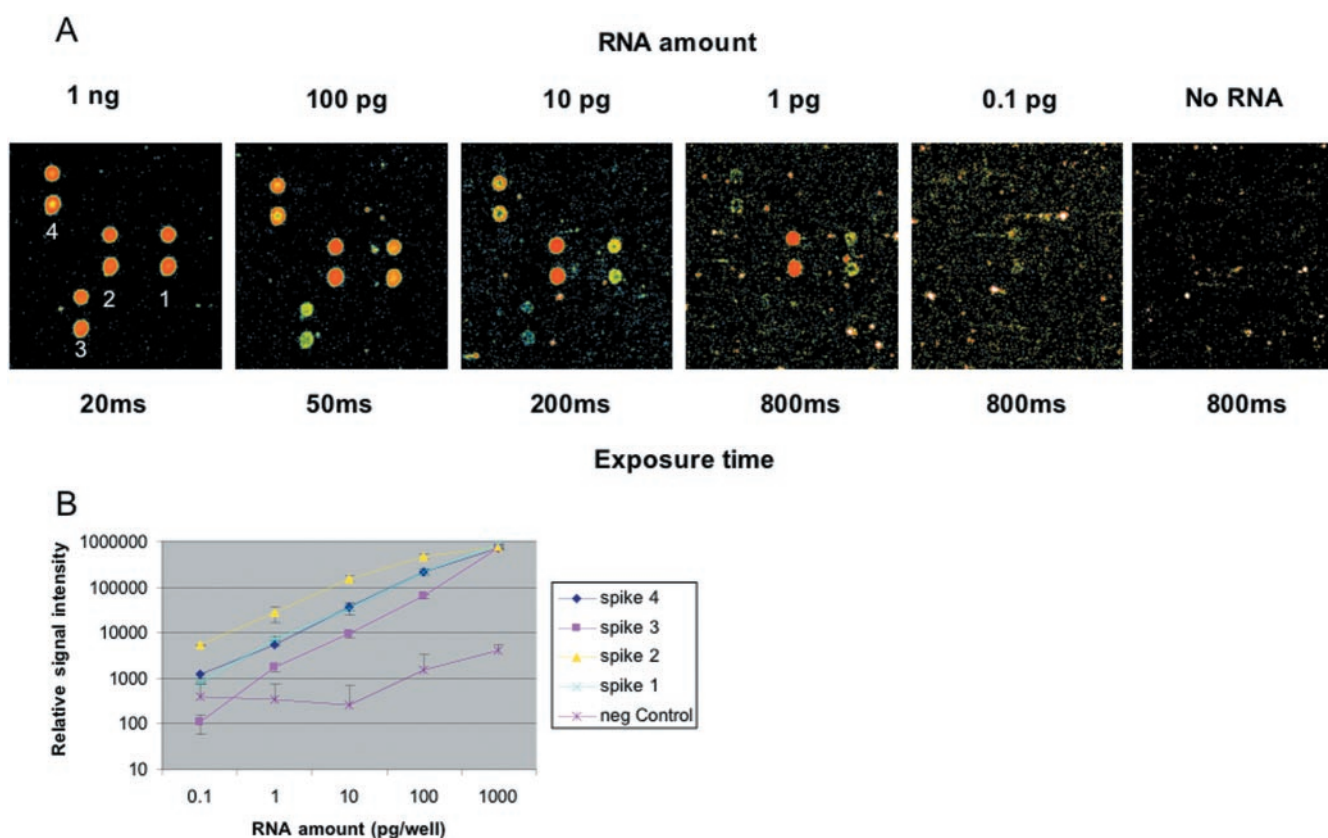


**Figure 2.** Sensitivity of the ClearRead™ expression system. (A) The scatter images of a target titration experiment using synthetic RNA from four bacterial genes. The bacterial RNA molecules possess an artificially added poly-A tail allowing their detection using the oligo-dT<sub>20</sub> detector probe. The amount of target ranged from 1 ng to 0.1 pg, as indicated. The corresponding exposure time used for imaging is given in milliseconds (ms) at the bottom of each image. (B) Data analysis of the bacterial RNA titration. Net signal intensities were obtained by subtracting the local background from mean signal intensities. The net signals were normalized based on their different exposure times and plotted in a log/log ratio. Two human captures for ubiquitin B and  $\beta$ -actin served as negative controls. The signals at these sites were averaged and normalized, and after adding 1 SD provided a threshold for a positive call. At 1 pg of target RNA, all four bacterial spikes show signals above the negative control. Below this concentration a distinct signal call was not possible.



carry up to 20 fluorescent labels, while we expect only a single silver complex to be generated at the poly-A tail of each mRNA, since even more than one nanoparticle in close proximity would probably result in a similar-sized gold-silver complex (unpublished observations). This multi gold-silver complex would exhibit similar scatter ability compared to a single gold-silver particle due to the same diameter of the aggregate. Therefore, varied lengths of poly-A tails within the mRNA transcripts are not expected to introduce variability in the signal strength.

### Linear range and dose response of scatter signals

In order to determine the dose response curve of the scatter signal imaged with the Verigene ID, we performed a human RNA target titration experiment (Figure 3A). The target amount for the dose response titration experiment ranged from 5  $\mu$ g to 5 ng in a 2 h hybridization. The net intensity values were normalized for the different exposure times used at varying RNA concentration, and plotted in a logarithmic scale (Figure 3B). The observed signal intensities for four genes (UBB, ACTB, RPL32, SARS) show a linear increase over 3 logs indicating a concentration-independent identification of the expression patterns. Additionally, this data

compares well to the reported dose response of fluorescent microarray hybridizations (22).

### Absence of 3' end bias

Enzymatic labeling and/or amplification steps with poly-T primed cDNA synthesis and their inherent 3' end bias of labeled products represent a major drawback of classical gene expression analysis, since the reverse transcription favors the generation of labeled products restricted to the 3' portion of a given mRNA population. This forces classical gene expression methods to design their capture probes close to the 3' end of the mRNAs. Based on the direct hybridization of unfragmented, total RNA employed in the ClearRead<sup>TM</sup> approach, we assumed that this reaction would not exhibit any bias regarding the position of the capture oligonucleotides. This hypothesis was tested with six capture oligonucleotides (50mer) complementary to sequences along the whole length (1793 nt) of the  $\beta$ -actin mRNA (ACTB). Hybridization experiments with total human mRNA revealed equivalent hybridization efficiencies for all six capture oligonucleotides (Figure 4), with only minor differences in signal intensities that are likely due to secondary structure-mediated variations in hybridization kinetics. These results support the finding of

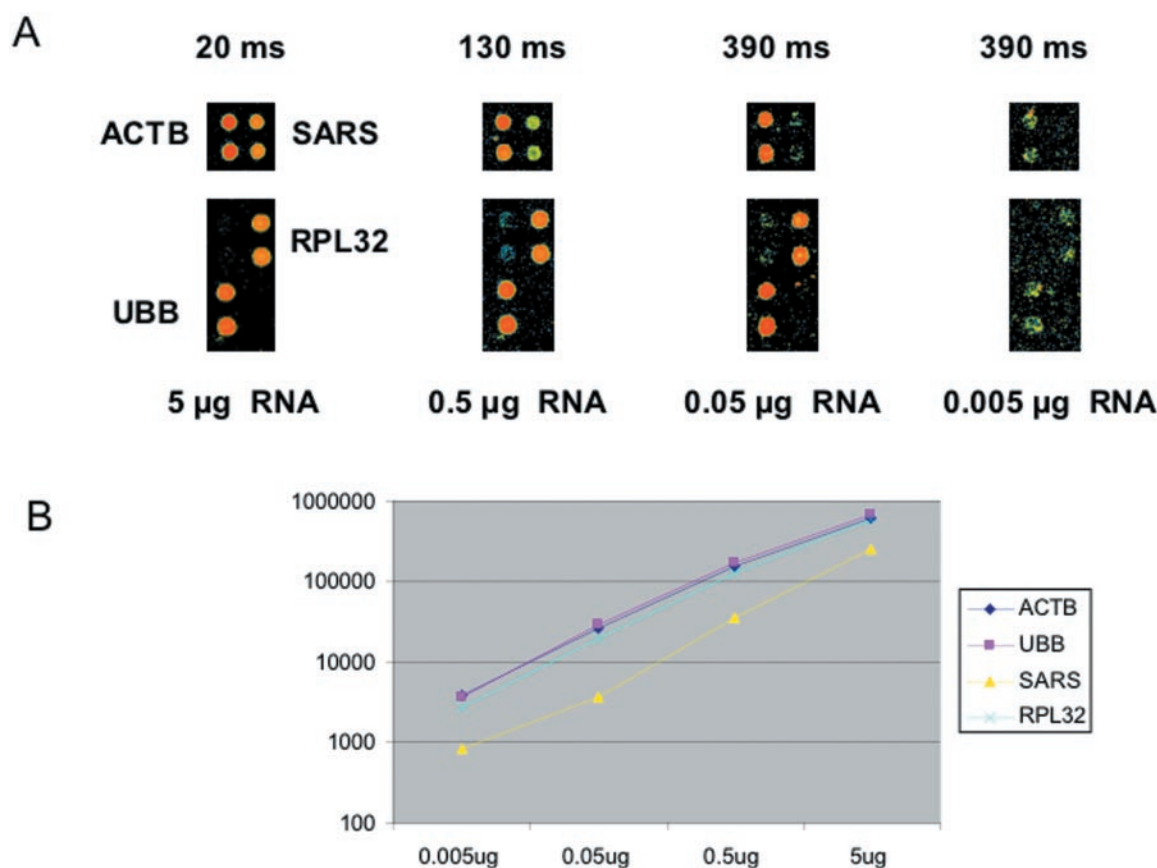


**Figure 3.** Linear dose response of scatter signals. (A) In order to assess the dose response curve for the ClearRead<sup>TM</sup> assay, a target titration experiment with the indicated amount of human RNA was conducted. Scanning exposure times in milliseconds are given above each image. Scatter signals of spots representing four human genes (ACTB, UBB, RPL32 and SARS) were analyzed. (B) Data analysis of the dose response titration. Net signals were normalized to the signals at the highest exposure time (390 ms), and the resulting relative signal intensities are plotted in a log/log ratio. All four analyzed genes show a linear dose response over 3 logs of target concentration.

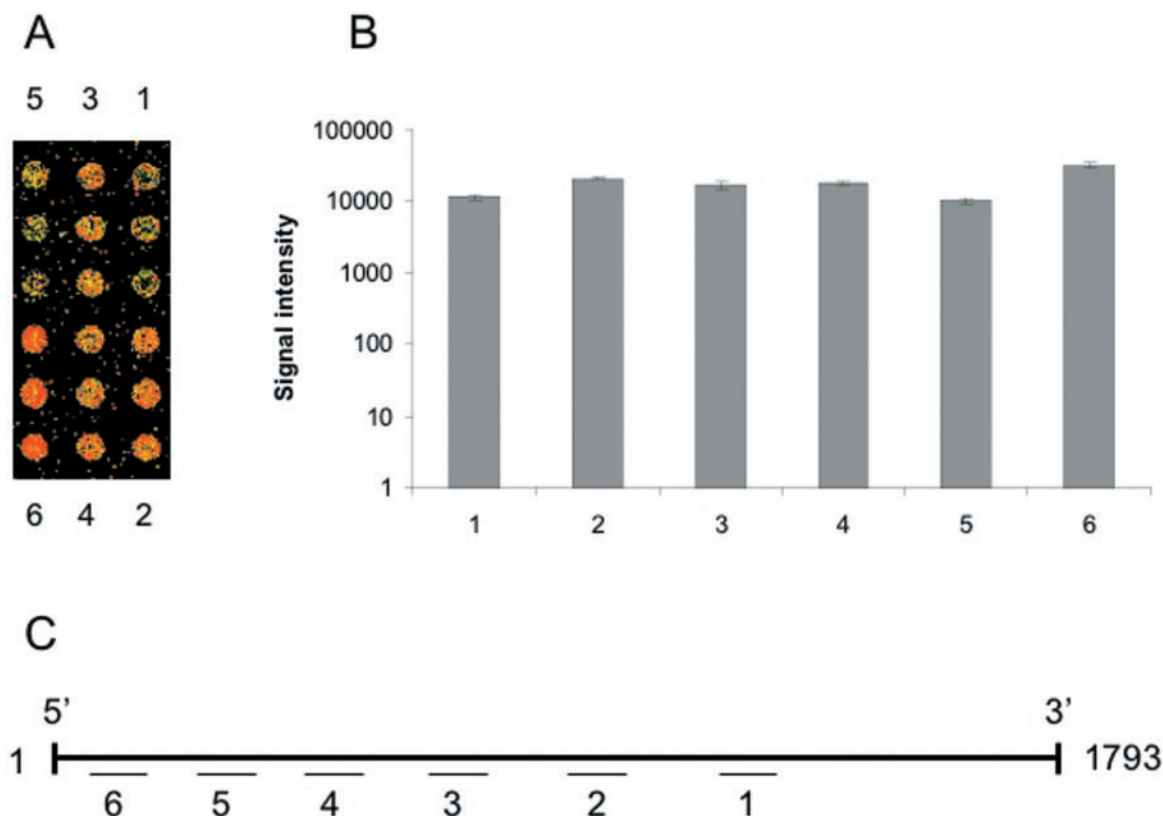


**Figure 4.** Absence of 3' end bias in ClearRead™ expression profiling. Six capture oligonucleotides were designed to be complementary to different sections of the β-actin mRNA (ACTB) as follows: Oligo1 (1051–1100), Oligo2 (781–830), Oligo3 (621–670), Oligo4 (461–510), Oligo5 (221–270), Oligo6 (74–123). The scatter image of hybridization with total human mRNA is shown in (A) and the corresponding data analysis in (B). The average mean signal intensities (corrected for local background) were plotted on a log scale. The error bars represent 1 SD. (C) Schematic drawing of the positions of the six capture oligonucleotides on the full-length β-actin mRNA.

Hagedoorn *et al.*, who demonstrated a lack of 3' end biased target preparation by direct chemical labeling and subsequent hybridization of the labeled RNA (23).

### Hybridization of total human RNA

We chose 13 human genes as a model system to test the concept of hybridizing total human RNA. These model genes represent high-, medium-, low- and non-expressed genes in brain tissue (according to expression levels reported in the GeneCard database: <http://bioinformatics.weizmann.ac.il/cards>). The relative expression levels, the name of each gene and the corresponding abbreviations are provided in Table 1. In a first experiment, a serial dilution of total human brain RNA ranging from 0.5 μg to 10 ng per 32 μl volume was hybridized to the array for 2 h at 40°C in a high-salt buffer, followed by washing and nanoparticle probe hybridization. As shown in Figure 5A, most hybridization signals are significantly above the negative control signals with an input of only 0.5 μg total RNA. Below this concentration, the capture spots for the low-level expressed genes lacked sufficient signal for quantitation, while the highly expressed genes were easily detectable (data not shown). A control experiment without target RNA showed no detectable signal at any spot. The four bacterial capture spots employed in the dose response experiment were used as negative controls. Their net signals

were averaged, and after adding 1 SD, the resulting values were used to define a threshold for a positive signal call (Figure 5C). Based on this threshold value, EPRS and CHAF1B were assigned 'not expressed' in brain tissue. Raising the target RNA concentration increased the signal for these genes only marginally, never exceeding the threshold value for a positive signal (data not shown). This finding is in agreement with data obtained by different expression analysis methods (see below).

### Comparison of ClearRead™ to other gene expression analysis methods

The validity of the ClearRead™ RNA expression results were assessed by comparison to mRNA expression levels reported in the GeneCard Encyclopedia of the Weizmann Institute of Science (<http://bioinformatics.weizmann.ac.il/cards>). The GeneCard Encyclopedia integrates a subset of biologically relevant information stored in major data sources, including gene expression data created by different methods. The entries in the database include gene expression levels from an Affymetrix gene chip system, SAGE (Serial Analysis of Gene Expression) and northern blot analysis, respectively (Figure 6). The expression profiles of 13 genes used in this study were compared to those measured by the methods in the database. Absolute signal intensities of the gold nanoparticle

probe-based expression analysis were normalized to the relative expression levels reported in the GeneCard database by dividing the averaged nanoparticle probe-based signal intensity of two housekeeping genes (ubiquitin B, UBB and

**Table 1.** The gene names and abbreviations used in this study

Gene	Relative expression in brain tissue	Annotation_US123
EPRS	Not expressed	Glutamyl-prolyl-tRNA synthetase
CHAF1B	Not expressed	Chromatin assembly factor 1, subunit B (p60)
OAZ1	Low	Ornithine decarboxylase antizyme 1
TCF3	Medium	Transcription factor 3 (E2A)
COX6C	Medium	Cytochrome c oxidase subunit VIc
HADHB	Medium	Hydroxyacyl-Coenzyme A dehydrogenase
G6PD	Medium	Glucose-6-phosphate dehydrogenase
AMPD2	Medium	Adenosine monophosphate deaminase 2
IARS	Medium	Isoleucine-tRNA synthetase
SARS	Medium	Seryl-tRNA synthetase
RPPL32	High	Ribosomal protein L32
ACTB	High	B-actin
UBB	High	Ubiquitin B
Bac spike4	n.a.	RNA spike 4
Bac spike3	n.a.	RNA spike 3
Bac spike2	n.a.	RNA spike 2
Bac spike1	n.a.	RNA spike 1

The relative gene expression retrieved from the GeneCard database were arbitrarily defined as follows: genes with relative expression values of  $\sim 1000$  were called high expressed, values  $>100$  were called medium expressed and  $<100$  were called low expressed. An expression value of  $\sim 10$  was the threshold for a positive signal call.

$\beta$ -actin, ACTB) by the relative expression level of the same genes reported in the GeneCard database. The resulting normalization factor was averaged and applied to the remaining genes leading to the relative expression levels shown in Figure 6. The observed variability of expression levels between the ClearRead<sup>TM</sup> expression system and the three other methods was found to be in the same range as the variability between these three classical expression analysis tools. Thus, direct use of total RNA target generates reliable data on the relative number of transcripts present in a given tissue.

### Reproducibility of the ClearRead<sup>TM</sup> assay

The inter-assay reproducibility of the ClearRead<sup>TM</sup> RNA expression method was evaluated by performing eight hybridizations (conducted by two operators) each with  $0.5 \mu\text{g}$  human brain RNA for 2 h at  $40^\circ\text{C}$ , followed by the poly dT<sub>20</sub>-nanoparticle probe hybridization. The average signal intensities subtracted by the local background are shown in Figure 7. The gene expression data reflects consistent values for the 13 human genes with the error bar displaying 1 SD of the signal intensities over eight arrays. The reproducibility of the assay is also mirrored in an average coefficient of variation (CV) of 0.27.

### DISCUSSION

DNA-modified gold nanoparticle probes offer promising new avenues for DNA diagnostics. Due to the high sensitivity associated with nanoparticle-induced scatter signal, we

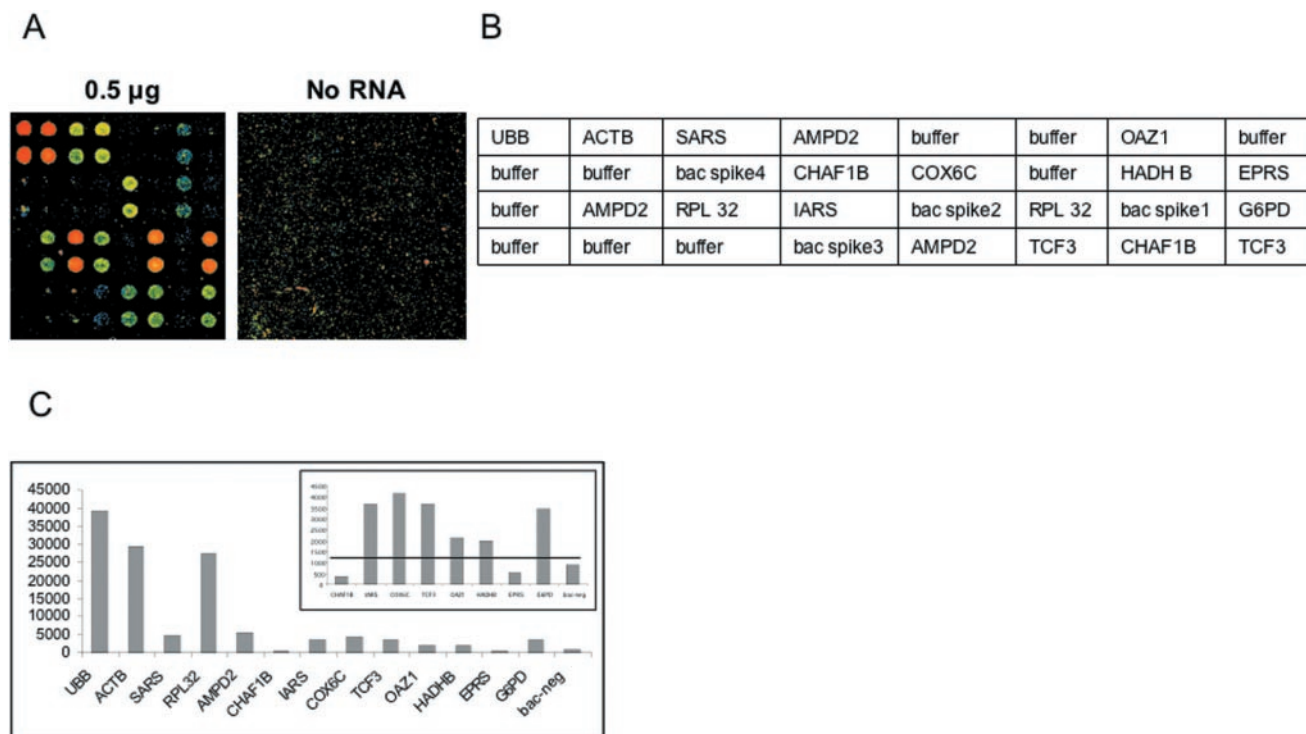


**Figure 5.** (A) Scatter images from a hybridization using  $0.5 \mu\text{g}$  total human brain RNA. The observed scatter signals (captured at 130 ms) are RNA dependent, as a control experiment without target shows no signal. (B) Schematic drawing of the array layout used in this study. Every capture was printed in vertical duplicates, i.e. every box of the layout represents two spots in a vertical arrangement. (C) Data analysis of the human RNA hybridization experiment. Shown is the plot of net signal intensities of every gene. The 'bac-neg' bar represents the average net signal (plus 1 SD) of the four bacterial spike captures, which served as a threshold value for a positive signal call. For clarity, the inserted plot shows the low-expressed genes and the negative control bar at a different scale of the y-axis. The threshold value for a positive signal call is shown as a horizontal black bar. The signals for EPRS and CHAF1B were below this threshold value and therefore assigned 'not expressed'.

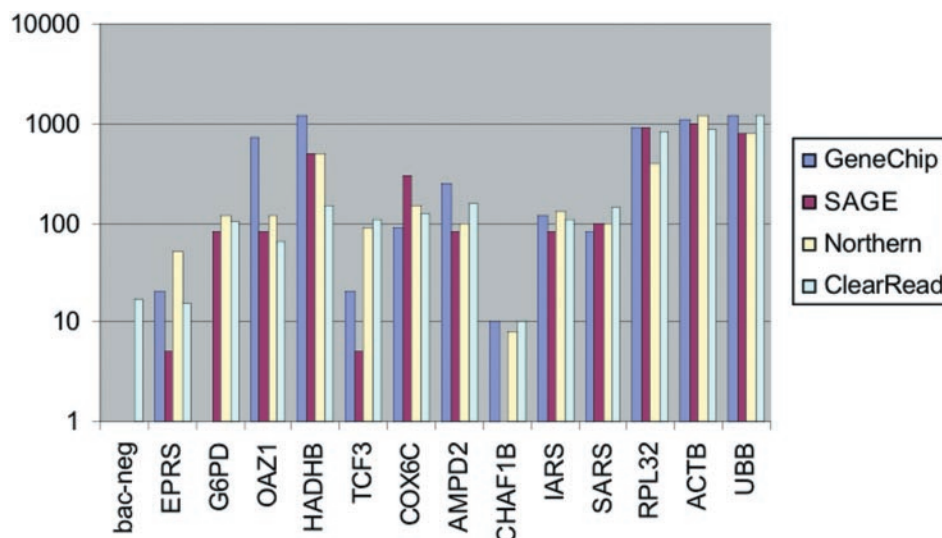


**Figure 6.** Comparison of expression values from the ClearRead™ system and entries from the GeneCard database. The relative gene expression values from the GeneCard database can be obtained by retrieving the individual GeneCards for every gene used in this study. The gene abbreviations used are identical to the names of the individual GeneCards. EPRS and CHAF1B with a relative expression value of  $\sim 10$  fell below the threshold of a positive signal defined by the relative signal of four bacterial control captures and was therefore correctly assigned 'not expressed' in brain tissue.

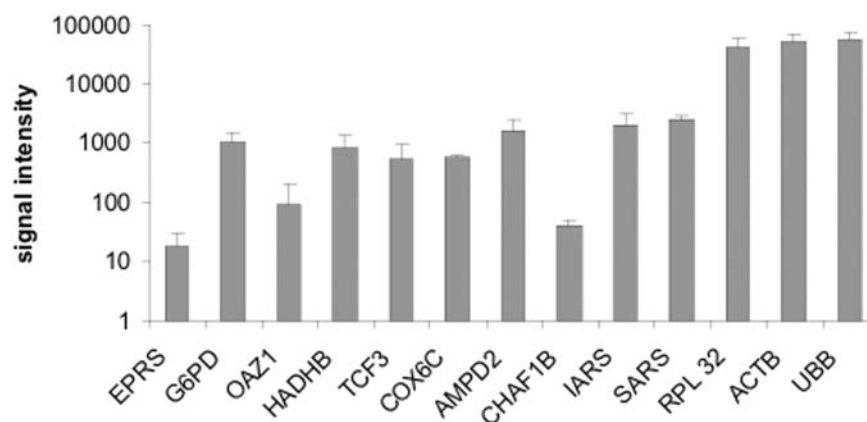


**Figure 7.** Average signal intensities of eight RNA hybridizations. The signal intensities (corrected for the local background) exhibit consistent values for the 13 human genes. The error bars indicate 1 SD of the signal intensities over eight arrays. The average coefficient of variation (CV) was calculated to be 0.27.

could recently demonstrate direct SNP detection from unamplified human genomic DNA (Y. P. Bao, H. Martin, T. F. Wei, S. S. Marla, J. Storhoff and U. R. Müller, manuscript submitted). Additionally, DNA-modified nanoparticles were shown to detect zeptomolar target sequences in a homogeneous colorimetric assay (24).

These promising results led us to investigate the usefulness of the powerful properties of nanoparticles in gene expression analysis. By targeting the poly-A tail of mRNA molecules, a 'Universal' detector probe in the form of an oligo-dT<sub>20</sub>-modified 15 nm gold nanoparticle probe could be employed, which eliminated labeling or target amplification steps. Avoiding the RT and IVT steps in target preparation simplifies the process and significantly reduces the overall assay time and cost. In a 2 h hybridization, 0.5  $\mu$ g of total RNA is sufficient to observe signals from genes with a known low-expression level (e.g. TCF3). In contrast, conventional fluorescent-based gene expression analysis usually requires an overnight

hybridization with 1–20  $\mu$ g of total RNA (or purified mRNA) as input, which eventually has to be amplified  $\sim 1000$  times by IVT before being applied to the microarray (10). Xiang *et al.* reported a novel approach using amine-modified oligonucleotides to prime cDNA synthesis, and claimed a sensitivity of 1  $\mu$ g total RNA; however, this method still relies on enzymatic conversion of the starting material and a 16–24 h incubation time (25). As expected, an extension of the hybridization time from 2 to 16 h also increases the hybridization sensitivity for ClearRead™ as well (data not shown), but we expect that for many applications the short assay time will outweigh the additional gain in sensitivity.

Recently, another nanoparticle-based gene expression analysis system was presented (GeniconRLS™, Invitrogen) (26), and demonstrated to be approximately 10-fold more sensitive in a direct comparison to fluorescence (27). However, the GeniconRLS™ system differs substantially from the method described in this paper. First, the Invitrogen approach utilizes



biotin-labeled cRNA, thereby requiring all the RT and IVT steps for target preparation and amplification as is the case for conventional analysis of gene expression. Second, the detection is accomplished by anti-biotin antibody-coupled gold and/or silver nanoparticles, whereas the ClearRead™ uses a universal oligo-dT<sub>20</sub>-modified gold probe that is directed toward the poly-A tail of mRNA molecules.

The demonstrated lack of a 3' end bias suggests an additional important advantage of the ClearRead™ assay in the analysis of splice variants. Alternative splicing is assumed to provide an explanation for the disparity between the modest number of human genes and the vast amount of gene products found in human cells. It is estimated that the transcripts of approximately 30% of all human genes are subject to alternative splicing (28). Since unfragmented RNA is used as target nucleic acid, and the position of the capture oligonucleotides do not adversely affect the hybridization efficiency, it seems feasible that splice variants can be detected and quantified with the method presented herein.

Additionally, the expression profiles generated by ClearRead™ agree well with those obtained by conventional expression analysis (Affymetrix gene chip, SAGE and northern blot analysis), indicating the ClearRead™ system is a reliable tool for measuring gene expression levels. Finally, the data generated in a small-scale reproducibility study points towards a solid assay with a low variability. It seems possible that this low variability is due to little hands-on time, originating from the lack of target labeling steps.

In conclusion, it appears that the ClearRead™ system could contribute substantially toward simplifying RNA expression analysis, paving the way for applications in the clinical environment.

## REFERENCES

- Lockhart,D.J. and Winzler,E.A. (2000) Genomics, gene expression and DNA arrays. *Nature*, **405**, 827–836.
- Iyer,V.R., Eisen,M.B., Ross,D.T., Schuler,G., Moore,T., Lee,J.C., Trent,J.M., Staudt,L.M., Hudson,J.Jr, Boguski,M.S. *et al.* (1999) The transcriptional program in the response of human fibroblasts to serum. *Science*, **283**, 83–87.
- Alizadeh,A.A., Eisen,M.B., Davis,R.E., Ma,C., Lossos,I.S., Rosenwald,A., Boldrick,J.C., Sabet,H., Tran,T., Yu,X. *et al.* (2000) Distinct types of diffuse large B-cell lymphoma identified by gene expression profiling. *Nature*, **403**, 503–511.
- Pomeroy,S.L., Tamayo,P., Gaasenbeek,M., Sturla,L.M., Angelo,M., McLaughlin,M.E., Kim,J.Y., Goumnerova,L.C., Black,P.M., Lau,C. *et al.* (2002) Prediction of central nervous system embryonal tumour outcome based on gene expression. *Nature*, **415**, 436–442.
- Perou,C.M., Sorlie,T., Eisen,M.B., van de Rijn,M., Jeffrey,S.S., Rees,C.A., Pollack,J.R., Ross,D.T., Johnsen,H., Akslen,L.A. *et al.* (2000) Molecular portraits of human breast tumours. *Nature*, **406**, 747–752.
- van 't Veer,L.J., Dai,H., van de Vijver,M.J., He,Y.D., Hart,A.A., Mao,M., Peterse,H.L., van der Kooy,K., Marton,M.J., Witteveen,A.T. *et al.* (2002) Gene expression profiling predicts clinical outcome of breast cancer. *Nature*, **415**, 530–536.
- Bhattacharjee,A., Richards,W.G., Staunton,J., Li,C., Monti,S., Vasa,P., Ladd,C., Beheshti,J., Bueno,R., Gillette,M. *et al.* (2001) Classification of human lung carcinomas by mRNA expression profiling reveals distinct adenocarcinoma subclasses. *Proc. Natl Acad. Sci. USA*, **98**, 13790–13795.
- Garber,M.E., Troyanskaya,O.G., Schluens,K., Petersen,S., Thaesler,Z., Pacyna-Gengelbach,M., van de Rijn,M., Rosen,G.D., Perou,C.M., Whyte,R.I. *et al.* (2001) Diversity of gene expression in adenocarcinoma of the lung. *Proc. Natl Acad. Sci. USA*, **98**, 13784–13789.
- Golub,T.R., Slonim,D.K., Tamayo,P., Huard,C., Gaasenbeek,M., Mesirov,J.P., Coller,H., Loh,M.L., Downing,J.R., Caligiuri,M.A. *et al.* (1999) Molecular classification of cancer: class discovery and class prediction by gene expression monitoring. *Science*, **286**, 531–537.
- Eberwine,J., Yeh,H., Miyashiro,K., Cao,Y., Nair,S., Finnell,R., Zettel,M. and Coleman,P. (1992) Analysis of gene expression in single live neurons. *Proc. Natl Acad. Sci. USA*, **89**, 3010–3014.
- Baugh,L.R., Hill,A.A., Brown,E.L. and Hunter,C.P. (2001) Quantitative analysis of mRNA amplification by *in vitro* transcription. *Nucleic Acids Res.*, **29**, e29.
- Han,E.S., Wu,Y., McCarter,R., Nelson,J.F., Richardson,A. and Hilsenbeck,S.G. (2004) Reproducibility, sources of variability, pooling, and sample size: important considerations for the design of high-density oligonucleotide array experiments. *J. Gerontol. A Biol. Sci. Med. Sci.*, **59**, 306–315.
- Kelly,J.J., Chernov,B.K., Tovastanovsky,I., Mirzabekov,A.D. and Bavykin,S.G. (2002) Radical-generating coordination complexes as tools for rapid and effective fragmentation and fluorescent labeling of nucleic acids for microchip hybridization. *Anal. Biochem.*, **311**, 103–118.
- Gupta,V., Cherkassky,A., Chatis,P., Joseph,R., Johnson,A.L., Broadbent,J., Erickson,T. and DiBeo,J. (2003) Directly labeled mRNA produces highly precise and unbiased differential gene expression data. *Nucleic Acids Res.*, **31**, e13.
- Cole,K., Truong,V., Barone,D. and McGall,G. (2004) Direct labeling of RNA with multiple biotins allows sensitive expression profiling of acute leukemia class predictor genes. *Nucleic Acids Res.*, **32**, e86.
- Cook,A.F., Vuocolo,E. and Brakel,C.L. (1998) Synthesis and hybridization of a series of biotinylated oligonucleotides. *Nucleic Acids Res.*, **16**, 4077–4095.
- Hentschel,C.C. and Birnstiel,M.L. (1981) The organization and expression of histone gene families. *Cell*, **25**, 301–313.
- Storhoff,J.J., Marla,S.S., Bao,P., Hagenow,S., Mehta,H., Lucas,A., Garimella,V., Patno,T.J., Buckingham,W., Cork,W.H. *et al.* (2004) Gold nanoparticle-based detection of genomic DNA targets on microarrays using a novel optical detection system. *Biosens. Bioelectron.*, **19**, 875–883.
- Grabar,K.C., Freeman,R.G., Hommer,M.B. and Natan,M.J. (1995) Preparation and characterization of Au colloid monolayers. *Anal. Chem.*, **67**, 735–743.
- Storhoff,J.J., Elghanian,R., Mucic,R.C., Mirkin,C.A. and Letsinger,R.L. (1998) One-pot colorimetric differentiation of polynucleotides with single base imperfections using gold nanoparticle probes. *J. Am. Chem. Soc.*, **120**, 1959–1964.
- Religio,A., Schwager,C., Richter,A., Ansorge,W. and Valcarcel,J. (2002) Optimization of oligonucleotide-based DNA microarrays. *Nucleic Acids Res.*, **30**, e51.
- Ramakrishnan,R., Dorris,D., Lublinsky,A., Nguyen,A., Domanus,M., Prokhorova,A., Gieser,L., Touma,E., Lockner,R., Tata,M. *et al.* (2002) An assessment of Motorola CodeLink microarray performance for gene expression profiling applications. *Nucleic Acids Res.*, **30**, e30.
- Hagedoorn,R., Joseph,R., Kasanmoentalib,S., Eilers,P., Killian,J. and Raap, A.K. (2003) Chemical RNA labeling without 3' end bias using fluorescent cis-platin compounds. *BioTechniques*, **34**, 974–976.
- Storhoff,J.J., Lucas,A., Garimella,V., Patno,T. and Müller,U.R. (2004) Homogeneous detection of unamplified genomic DNA sequences based on colorimetric scatter of gold nanoparticle probes. *Nat. Biotechnol.*, **22**, 883–887.
- Xiang,C.C., Kozhich,O.A., Chen,M., Inman,J.M., Phan,Q.N., Chen,Y. and Brownstein,M.J. (2002) Amine-modified random primers to label probes for DNA microarrays. *Nat Biotechnol.*, **20**, 738–742.
- Yguerabide,J. and Yguerabide,E.E. (2001) Resonance light scattering particles as ultrasensitive labels for detection of analytes in a wide range of applications. *J. Cell. Biochem.*, **37** (Suppl.), 71–81.
- Bao,P., Frutos,A.G., Greef,C., Lahiri,J., Muller,U., Peterson,T.C., Warden,L. and Xie,X. (2002) High-sensitivity detection of DNA hybridization on microarrays using resonance light scattering. *Anal. Chem.*, **74**, 1792–1797.
- Roberts,G.C. and Smith,C.W. (1902) Alternative splicing: combinatorial output from the genome. *Curr. Opin. Chem. Biol.*, **6**, 375–383.